Gaussian expansion approach to nuclear and Coulomb breakup

T. Egami,[1,][*] K. Ogata,[1] T. Matsumoto,[1] Y. Iseri,[2] M. Kamimura,[1] and M. Yahiro[1]

[1]*Department of Physics, Kyushu University, Fukuoka 812-8581, Japan*

[2]*Department of Physics, Chiba-Keizai College, Todoroki-cho 4-3-30, Inage, Chiba 263-0021, Japan*

We present an accurate method of simultaneously treating nuclear and Coulomb breakup of weakly bound nuclei by means of the method of continuum discretized coupled channels with the pseudostate method of discretization. As L^2-type basis functions of expansion of bound and continuum states of the projectile, we take complex-range Gaussian functions which in good approximation form a complete set in a large configuration space which is important for both nuclear- and Coulomb-breakup processes. The accuracy of the method is tested quantitatively for $^8\mathrm{B}+^{58}\mathrm{Ni}$ scattering at 25.8 MeV.

PACS number(s): 24.10.Eq, 25.60.Gc, 25.70.De, 26.65.+t

The method of continuum discretized coupled channels (CDCC) [1,2] has been successfully applied not only to reactions of weakly bound stable nuclei [3–10], but also to those of unstable nuclei [11–17]. Since accurate description of reaction mechanisms, including effects of projectile breakup, is necessary to derive information of incident nuclei from experimental data, CDCC plays a prominent role in the study of unstable nuclei. In all the analyses referred to above, CDCC describes the reaction system with a three-body model as shown in Fig. 1.

However, many unstable nuclei of current interest such as $^6\mathrm{He}$ and $^{11}\mathrm{Li}$ are known to consist of three clusters. For example, $^6\mathrm{He}$ is well described by the $^4\mathrm{He}+n+n$ model. In order to make detailed and systematic analyses of reactions with such nuclei, extension of CDCC to deal with four-body systems is essential.

Very recently, a new treatment of breakup continuum in CDCC was proposed [18], making use of pseudostate (PS) wave functions [1,19,20] obtained by diagonalizing internal Hamiltonian of the projectile with Gaussian basis functions [21]. For nuclear breakup processes, the method, hereafter referred to as PS-CDCC, was found to perfectly reproduce the "exact" breakup S-matrix elements $S(k)$ calculated by CDCC with the momentum-bin average (Av) method [1–3,22,23] for the breakup continuum (Av-CDCC). One of the most important advantages of the use of PS discretization is that one can easily construct an approximately complete set of internal wave functions of the projectile with a three-body structure within the configuration space that is important for the reaction process concerned. Therefore PS-CDCC with Gaussian basis functions makes it possible to perform the four-body CDCC analyses of projectile breakup, a preliminary result of which for $^6\mathrm{He}$ elastic scattering on $^{12}\mathrm{C}$, including effects of three-body nuclear-breakup channels of $^6\mathrm{He}$, has been published [24].

The four-body CDCC analysis mentioned above had the restriction that Coulomb breakup of the projectile was neglected. Obviously, however, the breakup processes are also important at energies below the Coulomb barrier. For example, the enhancement of the total reaction cross section for $^6\mathrm{He}+^{209}\mathrm{Bi}$ compared to $^6\mathrm{Li}+^{209}\mathrm{Bi}$ is considered to be due to the electric dipole transition of $^6\mathrm{He}$, which is absent in $^6\mathrm{Li}$ [25]. Thus, in order to make systematic analyses of reactions with three-body projectiles, inclusion of Coulomb breakup of the projectile in four-body CDCC is necessary.

However, question of the applicability of PS-CDCC to Coulomb breakup is quite nontrivial even for two-body projectiles. This is because the size of the coordinate space of the projectile needed to describe Coulomb breakup is much larger than that needed for nuclear breakup. For example, the maximum radius of the coordinate space is about 20 fm for nuclear breakup of d or $^6\mathrm{Li}$ [18], but about 100 fm for Coulomb breakup of $^8\mathrm{B}$ [16,17].

The purpose of this Brief Report is, as the first step toward the four-body CDCC analysis of nuclear and Coulomb breakup of three-body projectiles, to show that three-body PS-CDCC based on the Gaussian basis functions can well reproduce the result of three-body Av-CDCC for dissociation of two-body projectiles including both nuclear- and Coulomb-breakup processes. As for the test case we take $^8\mathrm{B}$ breakup from $^{58}\mathrm{Ni}$ at 25.8 MeV, which has intensively been analyzed by Av-CDCC including nuclear and Coulomb breakup channels [16,17,26].

Below we recapitulate the formulation of three-body CDCC; see Refs. [1,2,18] for the details. We assume that the $^8\mathrm{B}+^{58}\mathrm{Ni}$ scattering is described by the $p+^7\mathrm{Be}+^{58}\mathrm{Ni}$ system. The model Hamiltonian of the system is
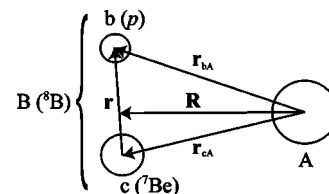
FIG. 1. Illustration of a three-body (A+b+c) system. The symbol B=b+c stands for the projectile and A is the target. In the calculation of $^8\mathrm{B}$ breakup by $^{58}\mathrm{Ni}$ shown below, b, c, B, and A are, respectively, p, $^7\mathrm{Be}$, $^8\mathrm{B}$, and $^{58}\mathrm{Ni}$.

---

*Electronic address: egami2scp@mbox.nc.kyushu-u.ac.jp

70 047604-1

$$H = K_r + V_{p\text{Be}}(\mathbf{r}) + K_R + U_{p\text{A}}(\mathbf{r}_{p\text{A}}) + U_{\text{BeA}}(\mathbf{r}_{\text{BeA}}),$$

where the coordinates are defined in Fig. 1 and the symbol A denotes the ^{58}Ni target. Operators K_r and K_R are kinetic energies associated with $\mathbf{r}$ and $\mathbf{R}$, respectively, and $V_{p\text{Be}}(\mathbf{r})$ is the interaction between p and ^{7}Be. The interaction $U_{p\text{A}}(U_{\text{BeA}})$ between $p(^7\text{Be})$ and A is taken to be the optical potential for $p+\text{A}(^7\text{Be}+\text{A})$ scattering. Coulomb breakup is induced by Coulomb components of the optical potentials. In this study, the intrinsic spins of the three constituents are neglected for simplicity.

In CDCC, the eigenstates of the $p+^7$Be system, i.e., the internal states of ^{8}B, are classified with the linear momentum k, the angular momentum ℓ, and its z component m of the system. In principle, the eigenstates consist of one bound state with $\ell=1$, i.e., the ground state of ^{8}B, and continuum states with the wave functions $\Phi_\ell(k,r)i^\ell Y_{\ell m}(\Omega_r)$ in which k and ℓ vary from 0 to ∞. In CDCC the continuum states are truncated by setting upper limits, $k_{\max}$ and $\ell_{\max}$, to k and ℓ, respectively. The truncation is the most basic assumption in CDCC, and it is confirmed for various projectiles that calculated S-matrix elements converge as $k_{\max}$ and $\ell_{\max}$ are increased [1,3,22]. The converged CDCC solution is the unperturbed solution of the distorted Faddeev equations, and corrections to the solution are negligible within the finite region of the r space and k space that is important for the reaction process concerned [27]. The continuum-state wave functions $\Phi_\ell(k,r)i^\ell Y_{\ell m}(\Omega_r)$ are then discretized into a finite number of wave functions, $\{\hat{\Phi}_{i\ell}(r)i^\ell Y_{\ell m}(\Omega_r); i=1-N\}$, each of which represents a "discretized-continuum state" with a certain positive eigenenergy labeled by i up to N. In CDCC, the resulting internal states of ^{8}B, consisting of the ground state and the discretized-continuum states, are assumed to form an approximate complete set in the finite region of the space that is important for the breakup reaction.

The three-body wave function Ψ_{JM} with the total angular momentum J and its z component M is expanded in terms of the approximate complete set. Coefficients of the expansion represent center-of-mass motions of ^{8}B in its bound and discretized-continuum states. Left-multiplying the three-body Schrödinger equation $(H-E)\Psi_{JM}=0$ by the internal states of ^{8}B, one obtains a set of coupled differential equations for the coefficients, hereafter called CDCC equations. Solving the CDCC equations with the appropriate boundary condition [1,2,22], we obtain the discrete breakup S-matrix element, $\hat{S}_{i\gamma,\gamma_0}$, for the transition from the initial channel with quantum numbers $\gamma_0=(\ell_0,L_0,J)$ to the ith discretized-continuum channel with $\gamma=(\ell,L,J)$, where $L(\ell)$ shows the orbital angular momentum regarding $\mathbf{R}$ ($\mathbf{r}$) in the breakup channel and the corresponding quantum numbers in the elastic channel are denoted by the subscript 0.

Discretization of the breakup continuum in the PS method is done by diagonalizing the internal Hamiltonian $H_{p\text{Be}}=K_r+V_{p\text{Be}}(\mathbf{r})$ in a space spanned by a finite number of L^2-type basis functions, for which we here take the following pairs of functions [21]:

$$\phi_{j\ell}^{\text{C}}(r) = r^\ell \exp[-(r/a_j)^2]\cos[b(r/a_j)^2],$$

$$\phi_{j\ell}^{\text{S}}(r) = r^\ell \exp[-(r/a_j)^2]\sin[b(r/a_j)^2] \quad (j=1-n),$$

where $\{a_j\}$ are assumed to increase in a geometric progression and $b=\pi/2$. We refer to the basis as the complex-range Gaussian basis, since the basis functions can be expressed by Gaussian functions with a complex-range parameter, $r^\ell \exp[-(1+ib)(r/a_j)^2]$, and its complex conjugate. The complex-range Gaussian basis functions oscillate with r, so they can simulate the oscillating pattern of the continuous breakup-state wave functions as shown in Ref. [21], which is very important for the description of Coulomb breakup by PS-CDCC. An accurate transformation from discrete $\hat{S}_{i\gamma,\gamma_0}$ to continuous $S_{\gamma,\gamma_0}(k)$ is possible, when the basis functions form an approximate complete set in the finite region of the r space and k space that is important for the breakup process [18]. The transformation has a simple form

$$S_{\gamma,\gamma_0}(k) = \sum_i \langle \Phi_\ell(k,r)|\hat{\Phi}_{i\ell}(r)\rangle \hat{S}_{i\gamma,\gamma_0}, \tag{1}$$

where $\langle\ \rangle$ denotes the integration over r and $\Phi_\ell(k,r)$ and $\hat{\Phi}_{i\ell}(r)$ are normalized as $\langle\hat{\Phi}_{i\ell}(r)|\hat{\Phi}_{i'\ell}(r)\rangle=\delta_{ii'}$ and $\langle\Phi_\ell(k,r)|\Phi_\ell(k',r)\rangle=\delta(k-k')$. The resulting $S_{\gamma,\gamma_0}(k)$, i.e., $S_{\gamma,\gamma_0}^{\text{PS}}(k)$, is smooth in the entire region of k.

In the Av method, on the other hand, the k continuum $[0,k_{\max}]$ for each ℓ is divided into a finite number of bins, each with a width $\Delta_{i\ell}=k_i-k_{i-1}$, and the continuum breakup-state wave function in the ith bin are averaged as follows:

$$\hat{\Phi}_{i\ell}(r) = \frac{1}{\sqrt{\Delta_{i\ell}}} \int_{k_{i-1}}^{k_i} \Phi_\ell(k,r)dk \quad \text{(for Av)}. \tag{2}$$

Here, the intrinsic energies of the states are defined by $\epsilon_{i\ell}=\langle\hat{\Phi}_{i\ell}(r)|H_{p\text{Be}}|\hat{\Phi}_{i\ell}(r)\rangle$. Inserting Eq. (2) into Eq. (1) leads to $S_{\gamma,\gamma_0}^{\text{Av}}(k)=\hat{S}_{i\gamma,\gamma_0}/\sqrt{\Delta_{i\ell}}$ for $k_{i-1}<k\leqslant k_i$ [13].

In order to see the applicability of three-body PS-CDCC for nuclear and Coulomb breakup, we calculated the breakup cross section of ^{8}B$+^{58}$Ni scattering at 25.8 MeV, and compared it with the result of Av-CDCC calculation. It should be noted that the Av-CDCC calculation with a large model-space [16,17] has succeeded in reproducing the experimental data [28] for the angular distribution of ^{7}Be fragment. For both the Av and the PS method, we took for ^{8}B the single-particle model of Esbensen and Bertsch [29]; here the depth of the potential was chosen so as to reproduce the separation energy of the proton, i.e., 137 keV, and the same potential was used also for the scattering states. We included only s and p states of ^{8}B to save the computation time. As for the distorting potentials for $p+^{58}$Ni and ^{7}Be$+^{58}$Ni, respectively, we took the potentials of Refs. [16,30]. CDCC equations were solved with the predictor-corrector Numerov method with stabilization [31]; here the matching radius was 500 fm and the maximum J was 1000.

In the Av-CDCC calculation, we took $k_{\max}=0.66$ fm^{-1} and $\Delta_{i\ell}=0.66/16\ (0.66/32)$ fm^{-1} for $\ell=1\ (0)$. The integration over r in the calculation of coupling potentials was truncated by setting an upper limit, $r_{\max}$, at 100 fm. The above model-space was found to give convergence of the resulting total
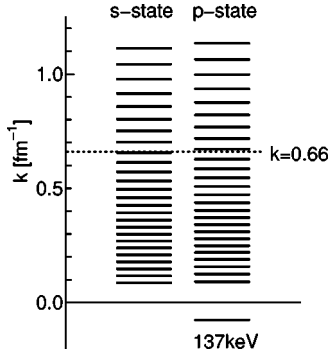
FIG. 2. Discretized momentum spectra of ^{8}B; the left (right) side corresponds to the s state (p state). The horizontal dotted line represents the cutoff momentum k_{max} taken to be 0.66 fm^{-1}.

breakup cross section. In order to obtain the correct asymptotic form of the Coulomb coupling potentials, we first rewrite the monopole components of them as

$$
\begin{aligned}
v_{i'\ell'i\ell}^{\mathrm{Coul}}(R) &\equiv C\left\{ \frac{1}{R}\int_0^{R/\beta_j} \hat{\Phi}_{i'\ell'}^*(r)\hat{\Phi}_{i\ell}(r)r^2 dr \right. \\
&\quad \left. + \int_{R/\beta_j}^{\infty} \frac{1}{\beta_j r}\hat{\Phi}_{i'\ell'}^*(r)\hat{\Phi}_{i\ell}(r)r^2 dr \right\} \\
&= C\left\{ \int_{R/\beta_j}^{\infty}\left(\frac{1}{\beta_j r}-\frac{1}{R}\right)\hat{\Phi}_{i'\ell'}^*(r)\hat{\Phi}_{i\ell}(r)r^2 dr \right. \\
&\quad \left. + \frac{1}{R}\delta_{i'i}\delta_{\ell'\ell} \right\},
\end{aligned}
\tag{3}
$$

where $\beta_j = 1/8$ $(7/8)$ for $j=p$ (^{7}Be) and $C=Z_j Z_{58_{\mathrm{Ni}}} e^2$; we have used the orthonormality of $\{\hat{\Phi}_{i\ell}\}$. Then, we put r_{max} to Eq. (3) as

$$
\begin{aligned}
v_{i'\ell'i\ell}^{\mathrm{Coul}}(R) &\approx C\left\{ \int_{R/\beta_j}^{r_{max}}\left(\frac{1}{\beta_j r}-\frac{1}{R}\right)\hat{\Phi}_{i'\ell'}^*(r)\hat{\Phi}_{i\ell}(r)r^2 dr \right. \\
&\quad \left. \times\, \theta(r_{max}-R/\beta_j)+\frac{1}{R}\delta_{i'i}\delta_{\ell'\ell} \right\},
\end{aligned}
\tag{4}
$$

which tends to Eq. (3) when $r_{max}\to\infty$.

In Eqs. (3) and (4), we used Coulomb interactions between two point charges for simplicity, while in actual calculations we took account of finite charge radii of ^{7}Be and ^{58}Ni. The result thus obtained with Av-CDCC is hereafter called the "exact" solution.

In the PS-CDCC calculation, we used the complex-range Gaussian basis with $(a_1=1.0,\ a_n=35.0,\ 2n=60,\ b=\pi/2)$ and took $r_{max}=130$ fm, which gave good convergence. Figure 2 shows the level sequence of the resulting discrete eigenstates, each with a discretized momentum $\hat{k}_{i\ell}$ defined as $\epsilon_{i\ell}=(\hbar\hat{k}_{i\ell})^2/(2\mu)$ by the corresponding eigenenergy $\epsilon_{i\ell}$, where μ is the reduced mass between p and ^{7}Be. One sees that the intervals of the $\hat{k}_{i\ell}$ are almost even. Thus the PS method well simulates the corresponding level sequence in the Av
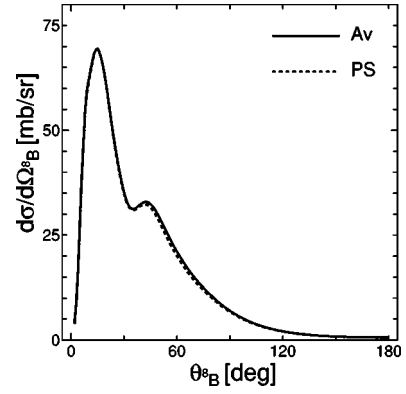
FIG. 3. Angular distribution of the total breakup cross section for ^{58}Ni(^{8}B,^{8}B*) at 25.8 MeV. The solid and dashed lines represent the results with the Av and PS methods, respectively.

method. This is also seen for the case of other projectiles [18]. The $\hat{\Phi}_{i\ell}(r)$ thus obtained turned out to oscillate up to about $r=100$ fm.

In actual PS-CDCC calculations, the discretized-continuum states with $\hat{k}_{i\ell}>k_{max}=0.66$ fm^{-1} had no effect on the result. So the PS-CDCC calculations were done with the truncation, that is, by taking 18 low-lying states for each of $\ell=0$ and 1. Thus the number of channels required by PS-CDCC was much smaller than that by Av-CDCC. As a consequence, the typical computation time with the former was about half that with the latter. This is an important merit of the use of the PS method.

We show in Fig. 3 the calculated angular distribution of ^{8}B total breakup cross section for ^{58}Ni(^{8}B,^{8}B*) at 25.8 MeV. The solid and dashed lines correspond to the Av and PS methods, respectively. One sees that the result
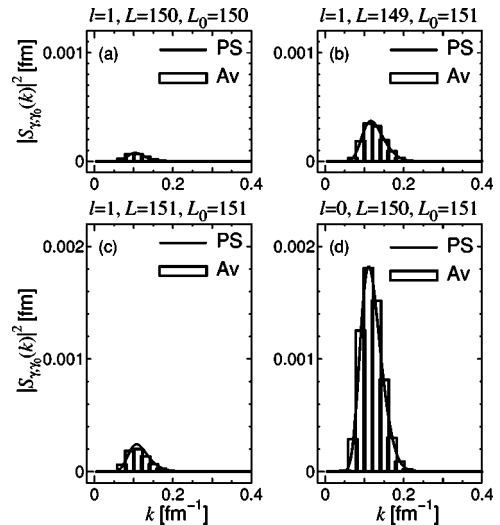
FIG. 4. The squared moduli of breakup S-matrix elements at $J=150$, as a function of k, for ^{8}B+^{58}Ni scattering at 25.8 MeV. Panels (a)–(d) correspond to $(\ell,L,L_0)=(1,150,150)$, $(1,149,151)$, $(1,151,151)$, and $(0,150,151)$, respectively. In each panel, the solid line represents the result of PS-CDCC, while the step line is the result of Av-CDCC assumed as the "exact" S-matrix elements. Other components not shown here are negligibly small.

with PS-CDCC almost perfectly reproduces that with Av-CDCC. It should be noted that our result in Fig. 3 agrees with that in Ref. [26] quite well; the disagreement is probably due to the small difference in the model-space used.

In order to see the validity of PS-CDCC for the ^{8}B nuclear and Coulomb breakup more precisely, we compared $S_{\gamma,\gamma_0}^{PS}(k)$ with $S_{\gamma,\gamma_0}^{Av}(k)$. In the calculation of the latter, the "exact" $S_{\gamma,\gamma_0}(k)$ was given with $\Delta_{i\ell}=0.66/32$ fm^{-1} for both the s and p states. This refinement made the k dependence of $S_{\gamma,\gamma_0}^{Av}(k)$ smooth but made no change in the elastic and total breakup cross sections.

Figure 4 shows the result of $|S_{\gamma,\gamma_0}(k)|^2$ at $J=150$ which corresponds to the elastic scattering angle of 10° when the classical path is assumed. The CDCC calculation with only Coulomb coupling potentials gave a peak at 10° in the total breakup cross section. One sees that the result of PS-CDCC (solid line) very well reproduces the "exact" solution (step line) for all k that is significant for the ^{8}B nuclear and Coulomb breakup.

In summary, three-body PS-CDCC proposed in Ref. [18] is shown to well describe nuclear and Coulomb breakup processes simultaneously. Because of the long range of the Coulomb coupling potentials, the model-space required for CDCC is very large. In particular, one must prepare the internal wave functions of the projectile, both in bound and continuum states, for a wide range of internal coordinate, say, 0–100 fm, which is in general difficult for PS methods. We find that this can easily be achieved by using the complex-range Gaussian basis, in the case of two-body projectile. The basis is also applicable to the reaction processes with three- and four-body projectiles, since energies and wave functions of the pseudostates of such projectiles are given easily [21]. Moreover, all coupled-channel potentials in four- and five-body PS-CDCC can be given analytically by the expansion of individual nuclear-optical potentials in terms of Gaussian functions. Thus we conclude that PS-CDCC based on the complex-range Gaussian basis functions is an effective method of practical use for nuclear and Coulomb breakup of three- and four-body projectiles.

[1] M. Kamimura *et al.*, Prog. Theor. Phys. Suppl. **89**, 1 (1986).

[2] N. Austern *et al.*, Phys. Rep. **154**, 125 (1987).

[3] M. Yahiro *et al.*, Prog. Theor. Phys. **67**, 1467 (1982).

[4] M. Yahiro *et al.*, Phys. Lett. **141B**, 19 (1984).

[5] Y. Sakuragi and M. Kamimura, Phys. Lett. **149B**, 307 (1984).

[6] Y. Sakuragi, Phys. Rev. C **35**, 2161 (1987).

[7] Y. Sakuragi *et al.*, Phys. Lett. B **205**, 204 (1988); Nucl. Phys. **480**, 361 (1988).

[8] Y. Iseri *et al.*, Nucl. Phys. **490**, 383 (1988).

[9] Y. Hirabayashi and Y. Sakuragi, Phys. Rev. Lett. **69**, 1892 (1992).

[10] K. Ogata *et al.*, Phys. Rev. C **67**, R011602 (2003).

[11] J. A. Tostevin *et al.*, Phys. Rev. C **66**, 024607 (2002); A. M. Moro *et al.*, *ibid.* **66**, 024612 (2002), and references therein.

[12] B. Davids *et al.*, Phys. Rev. C **63**, 065806 (2001).

[13] J. A. Tostevin *et al.*, Phys. Rev. C **63**, 024617 (2001).

[14] J. Mortimer *et al.*, Phys. Rev. C **65**, 064619 (2002).

[15] M. Takashina *et al.*, Phys. Rev. C **67**, 037601 (2003).

[16] N. Yamashita, Master thesis, Kyushu University, 2003.

[17] K. Ogata *et al.*, Nucl. Phys., **A738c**, 421 (2004).

[18] T. Matsumoto *et al.*, Phys. Rev. C **68**, 064607 (2003).

[19] A. M. Moro *et al.*, Phys. Rev. C **65**, 011602 (2002).

[20] R. Y. Rasoanaivo and G. H. Rawitscher, Phys. Rev. C **39**, 1709 (1989).

[21] E. Hiyama *et al.*, Prog. Part. Nucl. Phys. **51**, 223 (2003).

[22] R. A. D. Piyadasa *et al.*, Phys. Rev. C **60**, 044611 (1999).

[23] M. Yahiro and M. Kamimura, Prog. Theor. Phys. **65**, 2046 (1981); **65**, 2051 (1981).

[24] T. Matsumoto *et al.*, Nucl. Phys. **A738c**, 471 (2004).

[25] N. Keeley *et al.*, Phys. Rev. C **68**, 054601 (2003), and references therein.

[26] F. M. Nunes and I. J. Thompson, Phys. Rev. C **59**, 2652 (1999).

[27] N. Austern *et al.*, Phys. Rev. Lett. **63**, 2649 (1989); Phys. Rev. C **53**, 314 (1996).

[28] J. J. Kolata *et al.*, Phys. Rev. C **63**, 024616 (2001).

[29] H. Esbensen and G. F. Bertsch, Nucl. Phys. **A600**, 37 (1996).

[30] Z. Moroz *et al.*, Nucl. Phys. **A381**, 294 (1982).

[31] W. E. Baylis and S. J. Peel, Comput. Phys. Commun. **25**, 7 (1982).